RESEARCH ARTICLE

An application of computerized virtual landscape technology: Environmental landscape design

Dan Nie*

College of Fine Art and Design, Hubei Engineering University, Xiaogan, Hubei, China.

Received: May 29, 2024; **accepted:** August 22, 2024.

With the development of software technology and the improvement of scientific and technological levels, 3-dimensional (3D) virtual landscaping technology has played a pivotal role in landscape design research. To improve the intelligence level of the environmental landscape design, this study aimed to improve the computerized virtual landscape design by combining the idea of both box filter and Gaussian filter algorithms and replacing the Gaussian kernel function as the target kernel function in the box filter algorithm. The proposed system generated a set of scenes and supported a user-defined vegetation example model with its landscape of design (LOD), target landscape index, and a function for adapting natural conditions. The results showed that the filtering effect of the proposed algorithm was similar to that of the Gaussian filtering algorithm, which not only ensured the original filtering quality but also reduced the sampling of shadow maps' impact, thus the rendering efficiency was improved. The results confirmed that the proposed computerized virtual landscape technology positively affected environmental landscape design.

Keywords: virtual landscaping; environment; landscape design; panorama.

***Corresponding author:** Dan Nie, College of Fine Art and Design, Hubei Engineering University, Xiaogan, Hubei 432000, China. Email: niedan198209@163.com.

Introduction

The landscape design concept is a continuously deepening and developing research area. Landscape design originated in the United States of America in the 19th century and is a comprehensive discipline that integrates planning, design, transformation, restoration, and other interdisciplinary areas. Landscape design usually refers to the planning and designing of landscape and garden landscapes, and its core objective is to improve the living environments of human beings. It mainly includes two design perspectives including natural and artificial landscape elements [1]. Landscape design can transform a landscape into a higher aesthetic appreciation value, function as an ecological tool of sustainable development, and construct a relationship between human life and cities, residential areas, and various buildings and structures vividly and harmoniously. Urban landscape design is especially an important component of landscape design and a discipline dealing with comprehensive environmental construction in urban management, which deals with the environmental improvement of urban areas as the primary point and utilizes rich and diverse landscape design elements to blueprint the space of urban landscape that meets the material needs and spiritual pursuits of all levels

of a city [2]. Urban landscape design mainly utilizes various open urban spaces such as squares, urban roads, commercial blocks, and public environments such as parks and green spaces. Moreover, it adopts natural and artificial elements such as urban terrain, water system, vegetation, buildings and structures, public facilities, sculptures, and sketches as the main elements of landscape design and forms a livable urban space that meets the material life needs of the urban area. Hence, the pursuit of citizens' spiritual lives through a series of designs, combinations, and collocations can be enhanced [3].

With the rapid development and continuous expansion of urban constructions, linear landscape space can maximize the tolerance of the surrounding environment of construction and expand or narrow boundaries according to the needs, so the rare urban land resources can be protected to a certain extent. For example, the green landscape corridors and open urban spaces formed with the construction of linear landscape spaces can effectively enhance the value of land around them and stimulate further investment and urban construction. The linear landscape also provides protection and barriers for biological diversity and ecological environment to a certain extent and can prevent the destruction of the natural environment caused by the rapid construction of cities. Therefore, the construction of an urban linear landscape is an important guarantee for sustainable urban development and can maximize the protection and use of urban resources. Combining the linear landscape with slow-pace urban construction to form a linear slow-pace landscape design with urban characteristics can not only provide the basic functions of commuting and leisure activities for people but also protect the urban environment. Thus, historical and cultural relics can be restored, and urban characteristic resources and other diversified functions are better displayed. On the other hand, three-dimensional (3D) virtual landscaping technology has played a certain role in landscape design but has progressed gradually to respond to emerging and diversifying needs of landscape design. Landscape patterns can be divided into two mainstream thoughts of schools in Western countries, which includes the focusing on resource development, biodiversity conservation, and modeling data, and the concentrating on the influencing factors of landscape pattern evolution. Landscape pattern indices such as patch number, fractal dimension of perimeter area, average patch size, Shannon's diversity index (SHDI), and landscape area were selected to analyze the landscape pattern of Spanish cities [4]. Research methods at different scales were adopted to study landscape patterns and their evolution with different outcomes [5]. Those studies suggested that the temporal and spatial sensitivity of landscape led to spatial differentiation of landscape patterns. The spatiotemporal evolution laws of landscape patterns were then examined, simulated, and predicted with the future development of landscape patterns and suggestions [6]. However, with the acceleration of urbanization, the landscape pattern of cities has been disrupted. The research on landscape patterns has attracted scholars' attention. Geographic information science and technology were combined to select measurement indicators such as the number and area of embedded blocks, transfer matrix, dominance, and fragmentation to analyze the landscape pattern and explore the laws of dynamic changes in the landscape pattern [7]. A combination of geographic information systems and fractal statistics were combined to select indicators such as plate size, diversity, dominance, and fragmentation to examine the agricultural landscape pattern in the Loess Plateau of northern Shaanxi [8]. The characteristics and trends of urban spatial landscape patterns were investigated, and the different driving factors of landscape pattern alterations were derived [9]. Considered the level of socio-economic development influenced the evolution, while natural ecological conditions had a significant constraining effect, the data on green patches in the study area were collected and a fractal analysis of the landscape pattern

was conducted [10]. The results showed that the types of green spaces were not coordinated, and the layout was unreasonable. The analysis of the landscape pattern provides a reference for the planning of future developments. Satellite remote sensing images were also utilized to quantitatively analyze the landscape pattern characteristics of land use in the Yellow River Delta region through landscape indices, and the impact of related human activities on land use was pointed out [11]. Landscape pattern analysis and principal component analysis were employed concurrently to study the spatiotemporal evolution of wetland types and indices [12]. The exploration of spatiotemporal evolution is helpful to understand the relationship between disturbance factors in wetland ecology. In the study of landscape pattern evolution, qualitative description, conceptual extension, and landscape pattern data analysis are mainly focused, gradually moving qualitative research toward quantitative one.

In recent years, Convolutional Neural Networks (CNNs) have emerged and demonstrated strong capabilities in the field of computer vision, especially employing AlexNetTM. A series of deep learning networks such as VGG, Inception, and ResNe are employed in the field of image segmentation and recognition, while the shadow detection methods have been gradually developed. Deep learning algorithms are applied to the field of shadow detection, employing 2 distinct deep learning networks to extract the features of shadow regions and boundary regions, respectively, and conditional random fields to obtain results [13]. Conditional random field (CRF) optimization has opened the door to shadow detection algorithms based on deep learning. A fully CNN was employed to produce a prior shadow map and input the shadow feature map into a two-level cascaded network, achieving excellent shadow detection outcomes [14]. The shadow detector semantic colonization-based General Adversarial Network (ScGAN) predicted shadow maps by constructing a condition generator on an original input image. A deep network with a direction-aware spatial context module was developed to better utilize the extracted spatial semantic information to attain comprehensive image shadow features, greatly improving the effectiveness of shadow feature extraction [15]. A new shadow detection model was further proposed to investigate the contrast relationship between objects and shadow instances, further enriching the research direction of segmenting and pairing shadows and object instances together when the performance of shadow feature fusion was considered [16]. A dense feature map fusion structure was constructed, which fused feature maps generated by different convolutional layers and made progress in shadow image detection and restoration [17]. In the research of lightweight networks, the semantic pixel-wise segmentation (SegNet) model employed an encoding-decoding process and fewer parameters for end-to-end training [18]. The deep deconvolution network (DeconvNet) improved the capability of feature mapping based on SegNet and constructed a deep learning network with very few parameters to enhance the segmentation effect of images [19]. An algorithm employing depthwise separable convolution was proposed instead of implementing conventional convolution, which compressed the convolution computation while ensuring that each convolution channel contained image information [20]. The network was further optimized by introducing a reverse residual linear bottleneck structure based on the virtual cortex (V1), enabling the network algorithm to have efficient capabilities for image feature extraction while being lightweight, resulting in higher detection accuracy [21]. MobileNetV3, as a lightweight network, is one of the most excellent network models in the field of semantic segmentation. When compared to large deep learning networks, it has absolute lightweight advantages in terms of computation and parameter quantity, but also has the disadvantage of insufficient representation of some image detailed features in lightweight networks. Currently, 4 versions have been launched including DeepLabVl, DeepLabV2, DeepLabV3, and DeepLabV3+. Its main

advantage is the introduction of a resolution that can be arbitrarily controlled to derive features from the encoder, balancing accuracy and time through dilated convolution. In the encoding part, a dilated convolution is introduced, which increases the receptive field without losing information, allowing each convolution to output semantic information containing a large range of features [22].

Landscape design can create more value when computerized tools are adapted to all aspects of the process. Thus, more research should be directed to this area not only to benefit from this technology but also to generate better outcomes by balancing the needs of people and nature. This study aimed to improve the effect of environmental landscape design through computerized virtual landscaping technology. Through the combination of the proposed algorithm and a design system, the original filter quality was guaranteed while the necessary sampling of shadow maps was reduced. Hence, the rendering efficiency was improved. The results verified that the proposed computerized virtual landscape technology positively affected environmental landscape design.

Materials and methods

Development tools

OpenGL (OpenGraphics Library) (https://www.opengl.org) is a cross-platform graphic library implemented for high-performance 2D and 3D graphics rendering, which includes programming specifications for manipulating graphics and image functions. OpenGL has many functions including constructing 3D models, graphic transformations, image enhancement, bitmap display, color model indexing, setting lighting and materials, dual caching, and special image processing functions. Moreover, the OpenGL library includes various types of lighting processes and a set of mapping methods for object textures. By applying these techniques to image rendering and processing, the graphics rendering effect can be made more realistic. OpenGL also innovatively implements a dual cache mode, dividing different graphic processing into front-end and back-end caches, storing and calculating scenes, image generation, and final rendering results separately. Due to OpenGL containing an interface that does not rely on computer hardware, it can be easily ported and utilized on various popular platforms in the market. Many conversion functions inside can quickly and conveniently convert to 3DS/3DSMAX. The graphic designs produced by drawing software such as Pro/E and UG were converted into arrays in the form of model files, thereby converting image information into data for data crunching. The rendering pipeline, referring to the process of inputting the vertex sequence, color series, texture sequence, normal sequence, and other data of the model into OpenGL for Embedded Systems (OpenGLES) and outputting the screen, was the process of converting a series of 3D models into 2D graphics and outputting the screen. This process was divided into multiple steps, and the output of each step was the input of the next step. The rendering pipeline first processed the vertices in the scene, storing all vertices in the vertex buffer, and then sending the stored data to VertexShader (https://khronos.org) for matrix operations such as cropping, screen testing, primitive assembly, and rasterization. The operation results were then applied to texture calculation. When sampling textures in the scene, it was necessary to perform cropping tests in the fragment shader. A series of steps including alpha testing, template testing, depth testing, and mixing was taken followed by storing the calculations in a frame buffer, and finally employing OpenGL Application Programming Interface (API) for scene rendering. The overall OpenGL rendering pipeline was shown in Figure 1.

Box filter technology

The box filtering method approximates the filter directly by utilizing a linear combination of box functions with different sizes. The basic idea is to fit the target convolution kernel (usually bell-

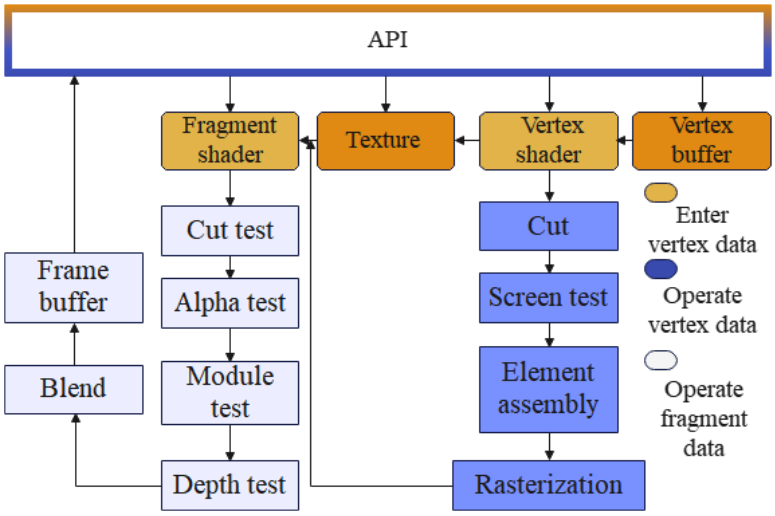

Figure 1. OpenGL rendering pipeline.

shaped) to the sum of weighted box-filtered maximum intensity projection (MIP) slices from the image pyramid (Figure 1), where unknown weights (w) need to be resolved. The algorithm is simple and effective, and the algorithm pipeline includes two stages of down-sampling and up-sampling. The main part of the algorithm is in the up-sampling stage. When filtering and sampling were run, the down-sampling phase employed a cartridge filter or other simple small convolution core cartridge filter to generate an ordinary image Mipmap. For the target kernel function $f(x)$, to generate a filtered Mipmap image, its pixel score was denoted by $p(L)$ under the current layer L. The algorithm linearly interpolated between a pixel sample $p(L+1)$ at a previously up-sampled rougher level and a sample $P_{down}(L)$ at a current level of the down-sampled image as shown in equation (1).

$$p(L)=(1-\alpha(L))\,p(L+1)+\alpha(L)\,P_{down}(L) \quad (1)$$

where m was a mixing parameter, which could be assessed by utilizing the weight of the box-filtered samples defined as below.

$$\alpha(L)=\frac{w(L)}{\int_L^m w(1)\,d1} \quad (2)$$

where m was the maximum MIP level score. L was the current number of layers. The ultimate goal of box filtering was to represent the target convolution of each pixel p by employing the weighted sum of $p_{box}(1)$, where $p_{box}(1)$ denoted the weighted sampling function that sampled the λ-th layer as equation 3.

$$p=\int_{\Omega} f(x)\,p_0(x)\,d\Omega=\int_0^m w(1)\,p_{box}(1)\,d1 \quad (3)$$

where $p_0(x)$ was the original sample offset x from the position of the pixel p. $w(1)$ was the weight of the box-filtered sample at the corresponding rank. $f(x)$ was the target kernel function. For the weighted sampling function $p_{box}(1)$ at level λ, the box filtering algorithm equaled it approximately to the sum of the original samples $p_0(x)$ within the box boundary, and the convolution was expressed as follows.

$$p_{box}(1)=\int_{\Omega} B(1,x)\,p_0(x)\,d\Omega \quad (4)$$

where $B(l,x)$ was the weight of the Mipmap of the l-th layer sampled. The generation method of Mipmap was to average every 4 pixels in the original image to generate pixels of the next layer, which was defined by equation (5).

$$B(l,x)=\begin{cases}4^{-l},\forall l\geq L\\ 0,\forall l<L\end{cases} \quad (5)$$

When equations (3), (4), and (5) were considered together, equation (6) was attained.

$$f(x)=\int_0^m w(l)B(l,x)\approx\int_L^m 4^{-l}w(l)dl \quad (6)$$

Therefore, the objective function $f(x)$ could be seen as an equivalent expression for the function $g(L)$ concerning the level L as below.

$$f(x)=g(L)\approx\int_L^m w(l)dl \quad (7)$$

When $g(m)=0$, $g(L)$ could be expressed by the definite integral of its derivatives as follows.

$$g(L)=-\{0-g(L)\}=-\int_L^m\frac{dg(l)}{dl}dl \quad (8)$$

The weight $w(l)$ was finally resolved by merging equations (7) and (8) to calculate the differentials on both sides using equation (9).

$$w(l)\approx-\frac{4^l dg(l)}{dl} \quad (9)$$

After obtaining the weight of the box filter samples at the level, the mixed parameters α were plugged into equation (1), and the final calculation was carried out to obtain the final result $p(L)$ of the linear interpolation of the upper and lower samples.

Improvement of VSM pre-filtering algorithm

After the shadow map was generated, the variance shadow map (VSM) algorithm (https://io7m.github.io/r2/documentation/p2s17.xhtml) could linearly filter the data stored in the shadow depth texture map. To blur the depth image and attain higher-quality soft shadows, Gaussian blurring and other filtering techniques were generally employed for filtering. Gaussian filtering adopted a full sampling method for the information of surrounding points in the sampling stage. The sampling rate was high, and the time consumption was relatively large. Therefore, a box filtering algorithm based on Gaussian filtering was added to divide the Gaussian filtering algorithm into two stages of upper and lower sampling, respectively, and assigned different weights to the sample in the sampling stage of Gaussian filtering. By reducing the sampling rate, the time consumption of the Gaussian filtering algorithm in the filtering stage was reduced. When Gaussian filtering was performed on a shading point *x* in a depth texture image, the pixels needed to be attained in the square area $R\times R$ around the colored point and then were multiplied by the Gaussian filtering function expressed by equation (10).

$$p(x)=\int_{R\times R}G(x,y)t(x,y)dxdy \quad (10)$$

where $G(x,y)$ was a 2D Gaussian filtering function. $t(x,y)$ was a sampling function of (x,y). Gaussian filtering had a good feature in that it could filter in the x direction first, and then filter in the y direction. Therefore, in the actual process, it was usually implemented for a 1D Gaussian filter function. In the sampling stage, the Gaussian filter needed to fully sample the pixels around the colored points. If it was assumed that the sampling radius of the Gaussian filter was $R=10$, then it was necessary to sample the square area 10×10 around the selected coloring point. It was necessary to sample the texture of the pixels around a coloring point 100 times. In the box-type filtering algorithm, the Mipmap generated in the down-sampling also contained a large amount of information about the pixels around the colored points and could be generated on the GPU at a low cost. Obtaining the information on the surrounding points from

the Mipmap to filter could greatly reduce the sampling rate and the required time. The filter was directly approximated by implementing a linear combination of box functions with different sizes. Therefore, this study proposed to add the box filter technology in the Gaussian filter to reduce the sampling rate to resolve the high sampling rate issues in the Gaussian filter. The 2 algorithms were then combined for algorithm analysis. The sampling weight of the Gaussian function was deduced mathematically by replacing the target kernel function $f(x)$ in equation (3) with a Gaussian function $G(x,y)$ to approximate the Gaussian filtering function $G(L)$ related to the hierarchy.

$$\begin{aligned} G(x,y) &= \frac{1}{2\pi\sigma^2} e^{\left(-\frac{x^2+y^2}{2\sigma^2}\right)} \\ G(x,y) = G(L) &= \int_L^m w(1) 4^{-1} d1 \\ G(L) &= \frac{1}{2\pi\sigma^2} e^{\left(-\frac{4^L}{2\pi\sigma^2}\right)} \end{aligned} \quad (11)$$

If the original function of $w(l)4^{-1}$ was $g(l)$, *i.e.* $g'(l) = w(l)4^{-1}$, then equation (12) was obtained as follows.

$$G(L) = \lim_{1\to\infty} g(1) - g(L) \quad (12)$$

In the up-sampling stage, the weight of the box filter should be closer to 0 as the number of layers was larger. Therefore, $\lim_{1\to\infty} g(1) = 0$ and the relationship $G(L) = -g(L)$ between box filtering and Gaussian filtering was deduced. The weight of the Gaussian filter was obtained by plugging equation (11) into equation (9) according to the relationship between the 2 algorithms.

$$w(1) = \frac{16^1 \ln 4}{4\pi^2\sigma^4} e^{\left(-\frac{41}{2\pi\sigma^2}\right)} \quad (13)$$

After obtaining the Gaussian filtering weights, equation (13) was assigned to 2 to obtain the mixing parameter $\alpha_{Gauss}(L)$ of the upper and lower sampling stages of the algorithm.

$$\alpha_{Gauss}(L) = \frac{w(L)}{\int_L^m w(1) d1} = \frac{16^L \ln 4}{2\pi\sigma^2\left(4^L + 2\pi\sigma^2\right)} \quad (14)$$

Through the derivation of the weight of the Gaussian filter function, the blending parameters would be implemented to compute the pixel samples $p(L)$.

System construction and testing

The three stages of the design generation device for a landscape plan required accessing different digital tools including a platform acquiring environmental information, a virtual mapping modeling platform and its simulation analysis plug-in, and a material entity control platform. The functions and principles of the commonly utilized platforms were presented in Figure 2 with Grasshopper as the core. When combined with the proposed algorithm, the collection, analysis, and utilization of data were realized, simplifying the response technology. The scope of installing environmental response was very extensive, and various elements of the landscape were contained to generate environmental response. From the perspective of design conception, response purpose was the primary nature of landscape installations. The environmental factor of response was the mapping condition of design, which affected and adjusted the form generation and state of landscape installation. Moreover, the component of the response landscape installation was the design object and the function object of mapping. The 3 elements of a single landscape installation constituted the method to respond to the environment as an environmental response design strategy (Figure 3). The information type and source in the stage of environmental information integration, the existence form and mapping method of environmental information in the virtually mapped modeling stage, and the methods and means of controlling each component in the

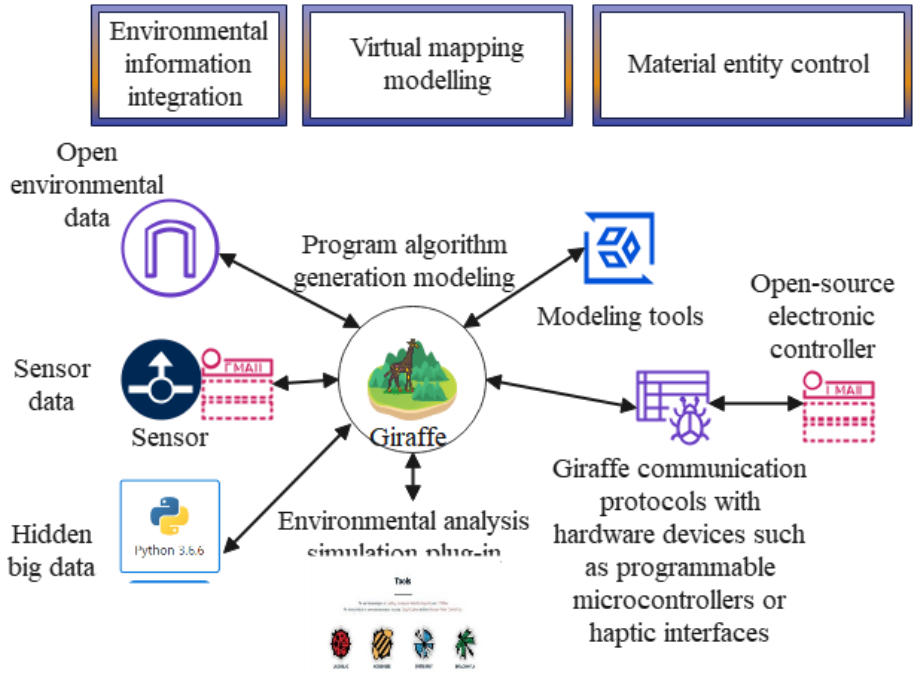

Figure 2. Tooling platform used in this study.

controlled material entity stage together constituted a digitally generated design mechanism based on environmental response (Figure 4).

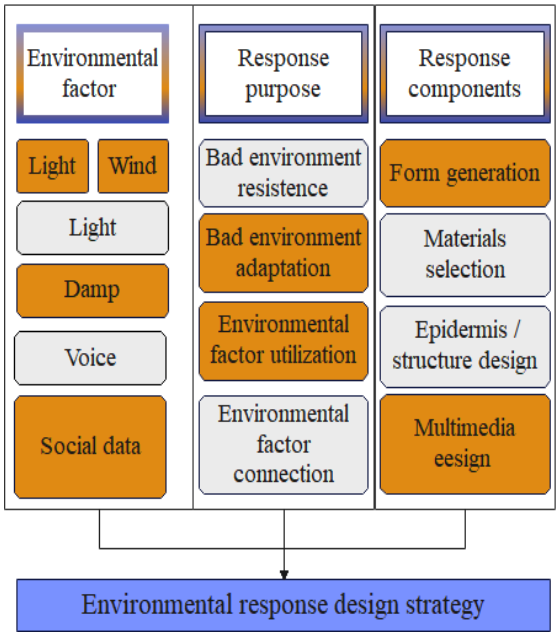

Figure 3. Components of an environmental response design strategy.

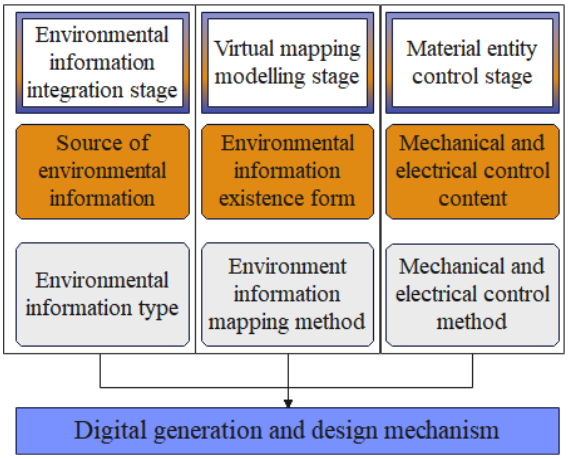

Figure 4. Components of digital generation design mechanism.

The implementation of computerized virtual imaging technology in environmental landscape design was summarized into 4 categories including environmental perception referring to the passive entity response generated by the direct contact between landscape device components and environmental factors; data mapping referring to obtaining real-time data of an indicator of environmental factors through

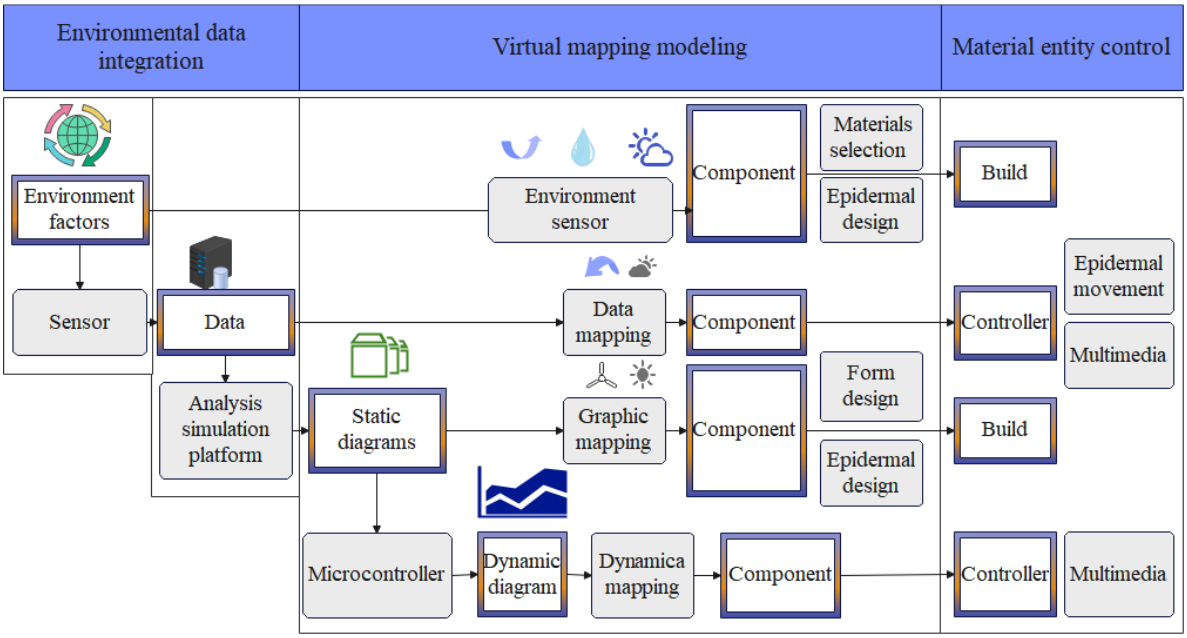

Figure 5. Action mechanism of environmental factors.

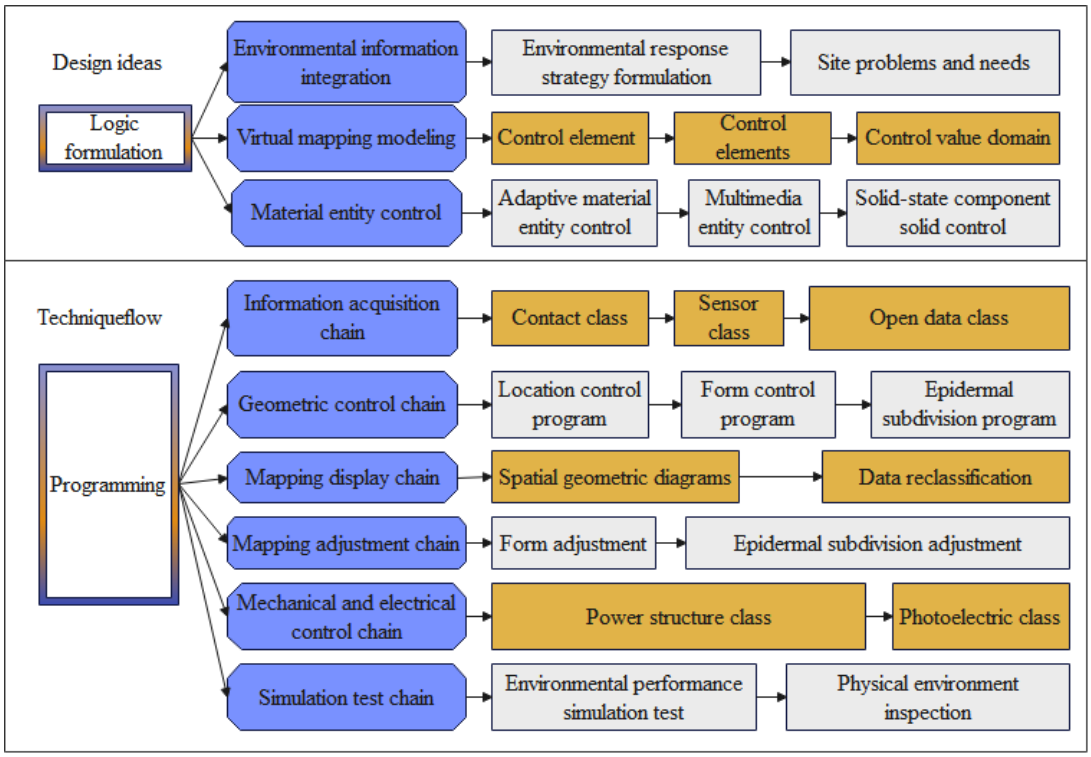

Figure 6. Workflow chart of digital generation design for environmental response of landscape installation.

sensors, reclassifying them, and mapping them to the active entity response of electromechanical control; graphical mapping referring to the static response generated by static graphical mapping

in the virtual modeling stage after the environmental data was professionally simulated and analyzed; dynamic mapping referring to the active response of the input controller to control the entity structure/skin parts by employing the diagram with temporal dynamics generated by the simulation software (Figure 5). The workflow mainly included 2 stages as logic formulation and programming (Figure 6). The logic formulation was the application of response thinking and a design idea that designers took the environmental status quo and the functional requirements of landscape installations as the primary point and carried out conditional constraints and rule formulation according to their subjective preferences. Programming was the process of converting the logical ideas formulated by the designer into code, which was the technical flow of landscape installation to achieve environmental response. The relationship between the two was sequential in time, that was, logic formulation determined the direction of code compilation that could test the rationality of logic formulation.

The experimental configuration was composed of AMD Ryzen 7 580 0x CPU, 64 GB memory, NVIDIA GeForce RTX 3090 GPU, Windows 11, Graph API OpenGL 4.6, Microsoft Visual Studio development tool, C++, OpenGL Interface, GLSL programming language.

Results and discussion

Based on an implemented scene generation system, which supported the user-defined vegetation model and its LOD, target landscape index, and natural condition adaptation function, the scene generation system could store all the vegetation prototype data in resource files for the real-time call of programmed scene generation and operation, which allowed users to reuse, modify, and manage various data conveniently. After running the roaming scene, the program would read the sprinkling results in the “Results” section and instantiate the vegetation information stored in the “Results” section in real-time in the view cone during the user's roaming. In this study, 2 different experimental scenarios were implemented, and the hierarchical VSM algorithm was implemented to compare and verify the proposed algorithm with the 2 different scenarios. The shadow rendering was performed on a static semi-closed simple scene under a simple forward light source in the first scene. In the room scene, there were multiple layers of walls to occlude the light source. When employing the layered VSM algorithm to paint shadows, the shadows formed on the ground should be completely black and should not produce bright gradient false artifacts. The effect of the proposed algorithm produced correct shadows when rendering this scene, it could effectively eliminate the issues available in the original algorithm. In the layering stage of the original algorithm, the study introduced the Lloydk-means clustering algorithm to determine the new layer segmentation points for uniform layering to achieve layer overlap and then employed the Chebyshev inequality in the conventional VSM algorithm to compute its visibility. The selection of the number of layers was very important, and different levels affected the final shadow effect. The results showed that, when the number of layers was uniformly constructed by increasing the segmentation points, the light gradient could be eliminated when the score was divided into about six layers. It was difficult to detect visually if the score was increased (Figure 7). The experimental rendering of the upper part was the linear variance shadow map (LVSM) algorithm (https://momentsingraphics.de/Media/HPG2017/32BitMSMSlides.pdf). Due to the incorrect layered computation of the closed wall, the shadow at the bottom of the scene had been affected. This part of the penumbra was superimposed on the original shadow, resulting in undue light leakage. In the picture, the bar-shaped light gradient artifact could be observed in the bottom area of the scene. During the experiment, the number of layers gradually increased into 2 layers, 4 layers, and 6 layers, respectively, but the correct shadow was still not produced (Figure 7A). Thus, the Lloydk-means

A.

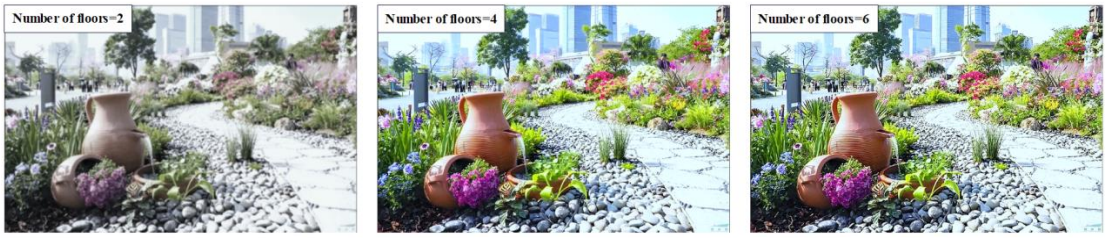

B.

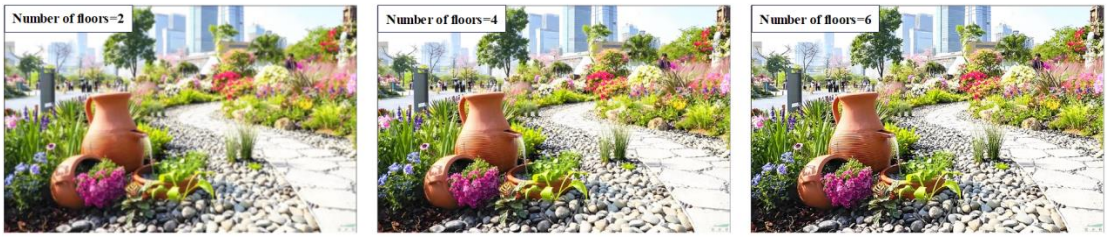

Figure 7. Elimination of illumination gradient. **A.** Elimination of lighting gradient. **B.** Using proposed algorithm.

A.

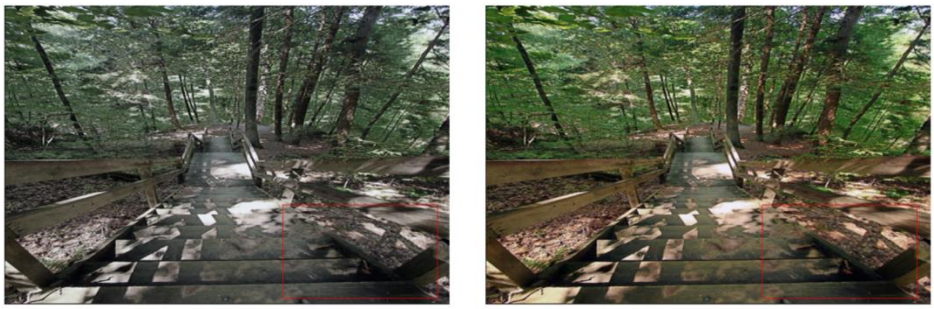

B.

Figure 8. Elimination of light gradient under different light directions.

clustering algorithm was introduced to improve the original algorithm. The uniform layering of the depth map was regarded as a 1D weighted clustering problem, and the position of layer segmentation points was retained according to the computed weights to achieve layer overlap. The results showed that, with the increase of the number of layers, the depth layer was overlapped by forming new segmentation points through the clustering algorithm. The depth distortion could be increased by increasing the interval of adjacent layers to form layer overlap.

Table 1. Model input landscape index.

	Target PLAND	Target AWMPFD	Target LPI	Target MPS	Exclusivity
Chinese fir forest	0.416	1.277	0.129	143.550	0.901
Hard and broad class	0.287	1.287	0.129	79.200	0.881
Eucalyptus	0.149	1.277	0.079	133.650	0.842
Pinus massoniana forest	0.059	1.287	0.010	44.550	0.723
Economic forest	0.079	1.307	0.010	49.500	0.703

Table 2. Landscape index of experimental results.

Landscape index	PLAND			AWMPFD			LPI			MPS		
Experimental serial number	1	2	3	1	2	3	1	2	3	1	2	3
Chinese fir forest	0.43	0.42	0.41	1.31	1.31	1.32	0.139	0.134	0.124	136	146	132
Hard and broad class	0.29	0.30	0.30	1.34	1.32	1.33	0.143	0.123	0.123	74	74	77
Eucalyptus	0.14	0.14	0.14	1.29	1.27	1.30	0.071	0.066	0.063	127	129	133
Pinus massoniana forest	0.06	0.05	0.06	1.34	1.27	1.33	0.014	0.010	0.014	41	40	41
Economic forest	0.08	0.08	0.09	1.28	1.32	1.32	0.012	0.017	0.012	45	47	42

Thus, it would not affect the visual effect of the overall shadow, and the light leakage phenomenon had been greatly reduced (Figure 7B). When the layer number was greater than six, the visual effect of altering parameters did not change much. When the number of layers was set to 6, the shadow formed on the ground by the closed area of the room in the scene was invisible due to the distortion.

For the second experimental scenario, the shadow rendering effect of the 2 algorithms showed the elimination of the illumination gradient artifacts formed by the 2 algorithms in different illumination directions in a dynamic scene. The shadow rendering effect of the LVSM algorithm in a dynamic scene demonstrated that, In the red box area, the illumination gradient artifacts were produced by different relationships of occlusions due to different illumination directions in the dynamic scene (Figure 8A). The correct shadow renderings produced by the proposed algorithm successfully eliminated the wrong artifacts in the original algorithm (Figure 8B). The results confirmed that the proposed algorithm still had strong practicability in dynamic scenarios. The percentage of patch area (PLAND) could most intuitively reflect the dominance of vegetation in the area and be directly obtained by dividing the grid numbers contained in the landscape type by the total grid numbers. The largest patch index (LPI) represented the degree of patch concentration. The larger the score, the larger the proportion of the largest patch area in the landscape type, and the smaller the intensity and frequency of disturbance. The average patch area (APS) could reflect the fragmentation of patches. Area weighted average fractal index (AWMPFD) reflected the complexity of patches in the same landscape element type. The larger the score, the greater the change of patch shape and the more complex the patch shape (Table 1). The corresponding landscape index when combined with the computerized virtual landscaping technology was shown in Table 2. Due to the natural conditions guiding the adaptation functions, landscape types could correspond to their appropriate elevation, slope, and other related information. It occupied the first place in PLAND and had the highest generation probability since each landscape type was specific. Chinese fir was easy to take the lead in the process of competitive growth of landscape patches. Therefore, the implementation could well simulate the clustering distribution of Chinese fir in the sample area and its distribution in other areas. In the same way, the hard-broad

class also reproduced the case of aggregating in the sample area and dispersing in the rest of the region. The dominant patch of *Eucalyptus* coincided with the sample area, but the other patches had a slightly weaker coincidence with the sample area, and there was a certain shift. The reason was that it formed a large competitive pressure with its adjacent Chinese fir, which forced the *Eucalyptus* to shift to its edge. In addition, the program could simulate the characteristics of economic forests mainly in low-slope and low-altitude areas. However, in addition to natural factors, economic forests were mostly affected by human activities, and the characteristic procedures of some patches along the road distribution could not be well simulated.

Linear landscape was first applied to the restoration of urban texture in the design of urban landscapes. The scattered functions of cities were connected with landscape nodes when combined with the needs of the natural landscape and social functions through the connection characteristics of linear space. As a new entry point and cognitive perspective of urban landscape design, it achieved a good display of natural landscape and human landscape based on protecting the natural environment, strengthening the construction of ecological civilization, and heritage restoration. In this study, computerized virtual landscaping technology was applied to environmental landscape design, and the box filter technology was analyzed and deduced mathematically. Moreover, the box-type Gaussian filtering algorithm was proposed and applied in the pre-filtering stage of the VSM algorithm, which reduced the sampling rate of the map without altering the rendering effect and thus improved the execution speed of the proposed algorithm. The results verified that the proposed computerized virtual landscaping technology had a good effect when applied to environmental landscape design in real settings. With the complexity and scale increased in scenes, the role of clustering algorithms in hybrid algorithms became more complex, which would lead to a sharp increase in the algorithm's complexity and a sharp decline in the algorithm's speed. Therefore, the problem of how to further improve the efficiency of the hybrid algorithm needs to be resolved in the future.

Acknowledgments

This study was supported by the Provincial First Class Curriculum Construction Project Phase Achievement "Landscape Design Method" (EJiaoGaoHan [2023] No. 19), Ministry of Education Industry-University Collaborative Education Project 2022 (Project Number: 220507022274203), and the "Residential Landscape and Planning Design" Gold Course Construction Project Phased Results (Project Number: 10528XJJK035).

References

1. Wang R. 2021. Landscape design of rainwater reuse based on the ecological natural environment: Hangzhou as an example. Arab J Geosci. 14(18):1877-1890.
2. Carbonell-Carrera C, Saorin JL, Melián DD. 2021. User VR experience and motivation study in an immersive 3D geo-visualization environment using a game engine for landscape design teaching. Land. 10(5):492-505.
3. Nikologianni A, Larkham PJ, Moore K. 2021. Built environment and landscape design as tools for resilient cities. AJA. 7(3):335-354.
4. Karandeev A, Sedykh O, Yartseva E. 2021. Assessing landscape design of small towns in Russia. Proceedings of the Institution of Civil Engineers-Urban Design and Planning. 174(3):116-130.
5. Wang Y, Chen L. 2022. Architectural and landscape garden planning integrated with artificial intelligence parametric analysis. Secur Commun Netw. 2022(1):1-9.
6. He M. 2020. The implementation and development of landscape design and ecological environment standardization in coastal residential areas. J Coast Res. 112(SI):55-58.
7. Zhang L, Xu H, Pan J. 2023. Investigating the relationship between landscape design types and human thermal comfort: Case study of Beijing Olympic forest park. Sustainability. 15(4):2969-2980.
8. Tang X. 2023. Research on intelligent landscape design based on distributed integrated model. Int J Semant Web Inf Syst. 19(1):1-19.
9. Cui W, Yang M, Zheng L, Xu T. 2020. Study on ecological landscape design in rural sewage treatment-taking Sanmenxia Lushi sewage treatment station as an example. Environ Eng Sci. 9(1):139-152.

10. Fekete A, Herczeg Á, Ge ND, Sárospataki M. 2022. Participatory landscape design and water management—a sustainable strategy for the renovation of vernacular baths and landscape protection in Szeklerland, Romania. Land. 11(1):95-102.
11. Zhang C, Li R, Dai L, Zhang P. 2022. Restoration of urban water environment landscape system and SWMM technology integration in water-scarce cities. Int Jst-T Civ Eng. 46(1):671-678.
12. Shan P, Sun W. 2021. Auxiliary use and detail optimization of computer VR technology in landscape design. Arab J Geosci. 14(9):798-810.
13. Karaca E, Karaca M. 2021. Environmental psychology approaches within the relationship of nature and health in terms of landscape architecture. Int J Knowl Soc Res. 18(42):5781-5802.
14. Shen X, Handel SN, Kirkwood NG, Huang Y, Padua MG. 2022. Locating the responsive plants for landscape recovery: A toolkit for designers and planners. Restor Ecol. 40(1):33-35.
15. Yinuo W. 2023. Research on landscape furniture design in Dongheqiao Village under the background of farming culture. Civ Eng Urban Plan J. 5(12):73-78.
16. Jahani A, Allahverdi S, Saffariha M, Alitavoli A, Ghiyasi S. 2022. Environmental modeling of landscape aesthetic value in natural urban parks using artificial neural network technique. MESE. 8(1):163-172.
17. Kamenečki M, Pletenac AM, Miholić H, Reljić DT, Krstonošić D, Pereković P. 2022. Revitalization and landscape design of the park in Stari Mikanovci, Croatia; the role of existing vegetation in generating new landscape solutions. AHR. 25(1):68-75.
18. Robinson JM, Jorgensen A. 2020. Rekindling old friendships in new landscapes: The environment–microbiome–health axis in the realms of landscape research. J People Nat. 2(2):339-349.
19. Liu J, Wu X, Zhang Y, Wang L. 2023. Visualization system of Hlai ethnic village landscape design based on machine learning. Soft Comput. 27:10001-10011.
20. Farooq S, Kamal MA. 2021. Analysis of landscape design and facilities in national bank park at Lahore, Pakistan. JACE. 9(2):386-393.
21. Staniewska A, Konopacki J. 2021. Minecraft games and public participation in landscape design–current teaching experience. WTE&TE. 19(2):238-243.
22. Chen H. 2021. Research on the application of productive agricultural landscape in urban residential areas. OALIB. 8(1):1-8.